Contact dependence of the conductance of H_2 molecular junctions from first principles

K. H. Khoo,[1] J. B. Neaton,[2] Hyoung Joon Choi,[3] and Steven G. Louie[1,2]
[1]*Department of Physics, University of California at Berkeley, Berkeley, California 94720, USA*
[2]*The Molecular Foundry, Materials Sciences Division, Lawrence Berkeley National Laboratory, Berkeley, California 94720, USA*
[3]*Department of Physics and IPAP, Yonsei University, Seoul 120-749, Korea*
(Received 27 July 2007; revised manuscript received 4 January 2008; published 17 March 2008)

Using a first-principles scattering-state approach, transport properties of molecular hydrogen in Pd and Pt junctions are computed, revealing a dramatic reduction in conductance when replacing Pt with Pd contacts. This decrease originates from a change in conduction mechanism, from ballistic transport in Pt junctions to off-resonance tunneling in Pd junctions. Our findings also indicate that lead atoms in contact with H_2 are as important in determining conductance as H_2 itself.

DOI: 10.1103/PhysRevB.77.115326 PACS number(s): 73.63.−b

I. INTRODUCTION

Recently, there have been several reports of measurements of the conductance of atomic-scale junctions formed from single atoms, atomic chains, and individual molecules using mechanically controllable break junctions and scanning probes.[1–8] For most organic molecular junctions where the molecule binds covalently to the metallic electrodes, the measured conductances are quite low, typically in the range $10^{-4}G_0-10^{-2}G_0$, and there is often significant disparity between measured experimental values and theory.[2,9–11] In contrast, for metallic point contacts and atomic chains, reported conductances are on the order of $1G_0$, significantly higher values arising from larger coupling between the molecule and the leads for states near the Fermi level, and there is a remarkable agreement between theory and experiment.[12–16] The disagreement for organic systems may be due in part to the extreme sensitivity of measured properties to the details of the metal-molecule contact geometry, an interface difficult to characterize experimentally and theoretically. Additionally, it is still far from clear whether standard theoretical frameworks, such as the density functional theory (DFT) as it is commonly applied, are effective for predicting conductance in such systems.[17–21] On the other hand, the more strongly coupled metallic point contacts are apparently in a regime where correlation effects are relatively less important, which would account for the good agreement between calculated conductances with experiment.

One might expect a fairly small conductance from junctions with a closed-shell molecule such as H_2, similar to that of organic molecule junctions, but the measured conductances for this "simple" molecule are reported to be surprisingly high, on the order of a conductance quantum, and agree reasonably well with theoretical results.[22–28] Smit *et al.* measured the conductance of a Pt break junction in a H_2 atmosphere at 4 K, and obtained a differential conductance of about one quantum unit, $G_0=2e^2/h$ at low bias. In the same study, shot-noise measurements suggest that the conductance is associated with a single channel, and inelastic tunneling spectra provide evidence that the H_2 molecule is involved and arranged in the junction with its bond axis aligned parallel to the transport direction, bridging the Pt contacts.[27] Following this experiment and also using break junctions, a different group measured the conductance of H_2 with Pd leads under similar conditions and reported a conductance value of only $0.3G_0-0.5G_0$, significantly less than the Pt case.[28] Given the similarity of the two metals, the reduction in conductance by a factor of 2 or 3 for Pd is surprising; the result was initially attributed to a drop in density of states due to a hydrogen doping of the Pd leads.[28]

Several recent theoretical calculations have corroborated the findings of the Pt experiment, giving large values of conductance of order of $0.1G_0-1.0G_0$.[23–26] Although two theoretical works are consistent with the hypothesis that Pd contacts have a lower conductance, no existing studies have adequately explained the mechanism for the sensitivity of the H_2 junction conductance to the choice of contacts. In this paper, we compute the transmission spectra and conductance of a single H_2 molecule connected to Pt and Pd (111) leads using an *ab initio* scattering-state method[29] and specifically examine how the choice of lead (or contact) affects the low-bias transport properties. We find that changing the contacts of a H_2 junction from Pt to Pd results in a significant decrease in electronic coupling between the molecule and contact and gives rise to a qualitative change in the conduction mechanism close to the Fermi level, consistent with the dramatic difference in the measured low-bias transport properties observed in the two cases.

II. METHODOLOGY

Equilibrium geometries in this work are calculated from first principles using DFT within the local density approximation (LDA) in a supercell that contains a hydrogen molecule plus 224 metal atoms.[30,31] The SIESTA package and localized pseudoatomic basis sets are used to obtain the ground-state properties.[32,33] For all structural relaxations, convergence is achieved by sampling four k points in the irreducible Brillouin zone of the supercell, while Γ-point sampling is employed for calculations utilizing the scattering-state formalism described below. We use a double ζ with polarization basis set for the hydrogen atoms, and double-ζ sp orbitals and single-ζ d orbitals for Pd and Pt.[32] The cutoff radii of the basis orbitals are determined by fixing the energy shift of atomic eigenvalues to 0.005 Ry, and the sampling of the real-space grid is controlled with an energy

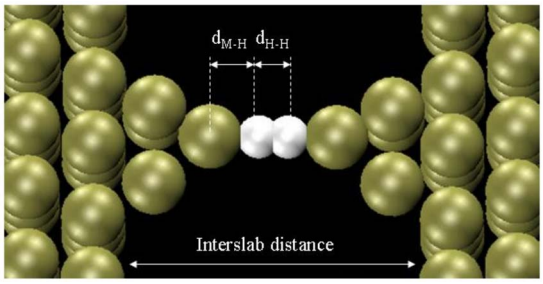

FIG. 1. (Color online) Model geometry used in conductance calculations: The H atoms are shown in white, and Pt or Pd atoms in gold. The interslab distance, H-H atom distance, and tip atom to hydrogen distance are determined by minimizing the total energy.

cutoff of 200 Ry.[33] The electron-ionic core interactions are represented by norm-conserving pseudopotentials.[34]

Electron transport properties are obtained using a coherent scattering-state formalism.[29,35] The H_2 molecule is first relaxed in a symmetric junction, with Pt or Pd leads attached on either side, and with translational symmetry imposed along directions parallel to the Pt or Pd surface. The junction is then partitioned into three regions: left bulk, center scattering region, and right bulk. The center scattering region is chosen to be sufficiently large so that the Hartree potentials at the left-center and right-center boundaries smoothly match those of the bulk. Here, we find three atomic layers on each side of the junction to be sufficient. Energy-dependent scattering states are constructed on a fine energy grid around the Fermi energy,[29] with incoming and outgoing itinerant and evanescent states determined from the bulk lead (Pt or Pd) complex band structure.[29,36] Typical energy grid spacings used in this work are 5 meV. This results in a linear system of equations at each energy E, which are solved to yield transmission matrix t with elements $t_{nm}(E)$ for each incoming channel n and outgoing channel m. The zero-bias conductance is then computed from the Landauer formula $G/G_0 = \mathrm{Tr}(t^{\dagger}t)$, where t is evaluated at E_F.[37]

III. RESULTS

We consider a geometry in which the H_2 molecule, with its bond along the transport axis, is placed between two metallic pyramid tips, similar to previous works.[23–25] The pyramids are connected to planar (111) metallic leads, as shown in Fig. 1. The central scattering region consists of three slab layers on either side of the junction, with additional three slab layers for both the left and right bulk lead regions. This gives a total of 12 slab layers plus the junction, for a total of 226 atoms inside the simulation supercell.

This choice of junction geometry is motivated by several factors. First, the vibrational frequencies of H_2 computed with this geometry are consistent with inelastic tunneling spectroscopy peak energies measured in break-junction experiments.[27] Second, shot-noise measurements suggest that the conductance is carried by a single channel, consistent with previous calculations for a linear geometry.[23–25] Third, the linear geometry is reported to be favored just before breaking for junctions under tension.[23] In addition, pyramidal junction geometries have been observed previously with transmission electron microscopy and in molecular dynamics simulations of nanowire formation.[38,39]

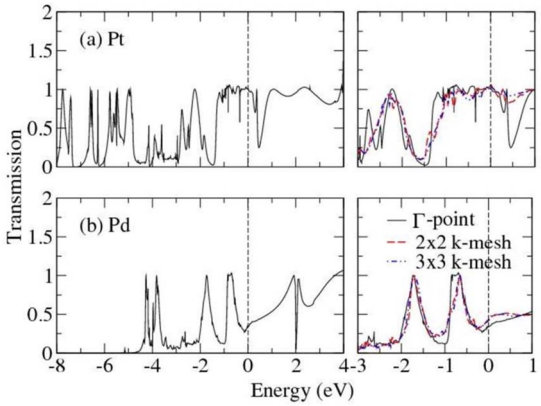

FIG. 2. (Color online) Transmission spectra for H_2 junctions across planar (a) Pt (111) and (b) Pd (111) leads. Left panels show transmission spectra obtained from Γ-point calculation, and dotted lines indicate the position of E_F. Right panels show a comparison between transmission spectra obtained with different k-grid samplings.

The determination of our optimized junction geometry proceeds in two steps. First, the top two layers of an isolated, six-layer metallic slab with bulklike interatomic distances are relaxed. We use theoretical lattice constants obtained from LDA calculations using the basis set described in Sec. II for bulk leads, 3.83 and 3.88 Å for Pd and Pt, respectively. After relaxing the isolated Pt slab, we observe an increase for the topmost interlayer spacing, while the corresponding distance in Pd slabs showed negligible change. Our results are similar to those obtained in earlier calculations of the (111) surfaces of these metals.[40,41] The junction is then formed by positioning the relaxed slabs on either side of atomic pyramids connecting a H_2 molecule. The pyramid atoms and H_2 are allowed to relax completely at several interslab separations, from which we select the one with the lowest overall energy after relaxation.

Following the procedure outlined above, the equilibrium hydrogen bond lengths within the junction are 0.88 Å (Pd leads) and 0.99 Å (Pt leads). Both bond lengths exceed that of isolated H_2, calculated to be 0.76 Å within the LDA. This significant lengthening of the H_2 bond suggests a strong interaction between the metal tip atom and H_2, with the Pt tips interacting more than Pd. The tip-to-hydrogen distances are calculated to be 1.71 Å with Pd leads and 1.68 Å with Pt leads. Increasing the interslab distance (from equilibrium) results in H_2 dissociation for Pt-H_2 junctions and desorption for Pd-H_2 junctions, again consistent with a significantly stronger lead-molecule coupling in the Pt junctions.

Using the relaxed atomic coordinates of the junction, we calculate the Γ-point zero-bias transmission spectra, and the results are shown in the left panels of Fig. 2. Interestingly, the transmission does not exceed unity, the maximum value expected for a single spin-degenerate channel, over the entire energy range. For both Pt and Pd junctions, there are sharp

resonant peaks at energies more than 4 eV below the Fermi level, a range coincident with the *d* bands in the metallic lead. For energies close to and above the Fermi level, there is an increasing contribution to the conduction from relatively delocalized *s*-like lead states, and these give rise to broader transmission features due to stronger hybridization and larger overlap with the junction. The Pt spectrum has a conductance plateau of about $1.0G_0$ over a range of several eV around the Fermi level, and a robust zero-bias conductance value of one quantum unit, in agreement with the experimentally measured value and a previous calculation.[24] For Pd leads, the transmission [Fig. 2(b)] differs noticeably from that of the Pt case near the Fermi level: A resonance peak appears just below E_F, and the transmission gradually rises from 0.35 at the Fermi level to 1.0 at 2.0 eV above E_F. The calculated conductance for H_2 with Pd leads is $0.35G_0$, appreciably less than the Pt case but consistent with experimental conductance.[28] As a check of convergence, calculations were also performed for the 2×2 and 3×3 *k*-mesh samplings perpendicular to the transport axis. Transmission spectra calculated with a 2×2 *k* mesh are qualitatively similar to those obtained from Γ-point calculations, as can be seen in the right panels of Fig. 2, and the conductance of the Pt junction remains at $1.0G_0$ while that of the Pd junction increases slightly from the Γ point value of $0.35G_0-0.42G_0$. Increasing the *k* mesh from 2×2 to 3×3 increases the conductance by less than $0.01G_0$ for both Pt and Pd junctions, indicating quantitative convergence. These transmission spectra show that Γ-point calculations are sufficient to capture the essential physics driving transport behavior in these junctions, allowing us to consider only Γ-point results in our subsequent analysis.

To gain further insight, we decompose the incoming lead states into independent eigenchannels by diagonalizing the matrix $t^\dagger t$, where $t=t_{nm}(E)$ is an energy-dependent matrix composed of the transmission coefficients of the scattering-state wave functions.[42] The eigenvectors of $t^\dagger t$ are the eigenchannel wave functions, and the contribution of each eigenchannel to the transmission value at a particular energy is the corresponding eigenvalue. For both Pt-H_2 and Pd-H_2 junctions, we find after diagonalization that a single eigenchannel dominates the transmission spectrum over a wide range of energies about the Fermi level.[25,43] This is due to the fact that the projected density of states (PDOS) on the H_2 molecule has a dominant antibonding character near E_F, reducing the number of junction conduction channels across H_2 to 1.

IV. DISCUSSION AND ANALYSIS

To understand the difference between the Pt and Pd spectra in Fig. 2, we analyze the transmitting eigenchannel wave functions (defined to be the eigenchannel with the highest eigenvalue) at E_F in real space. Contour plots for both Pt and Pd junctions are shown in Fig. 3, which show a superposition of incident, reflected, and transmitted waves.

For the Pd junction, strong reflection is evident at the lead tip atom, resulting in relatively less weight on the right side of the junction. For the channel with the only non-negligible eigenvalue, we observe a near-perfect transmission (i.e., eigenvalue near unity) for the Pt junction but only a partial transmission for the Pd junctions, consistent with the calculated conductance in each case. It is important to note that for the Pd-H_2 junction, reflection of the incident electron occurs primarily between the tip atom and pyramid base, strongly suggesting that the H_2 molecule is not solely responsible for the drop in conductance in the Pd case. To explore this further, we use the Friedel sum rule to relate the transmission $T(E)$ and scattering phase shift to the partial density of states of the junction and examine the spatial region relevant to electron transport for these junctions.[44] We find that the phase shifts induced by an "extended molecule," a four atom unit that we define to consist of the H_2 molecule and its two adjacent metal tip atoms, are sufficient to reproduce the transmission spectra at E_F for both Pt-H_2 and Pd-H_2 junctions,[45] while phase shifts from H_2 alone are not, a result that suggests that the tip atoms play a significant role in determining the junction conductance.

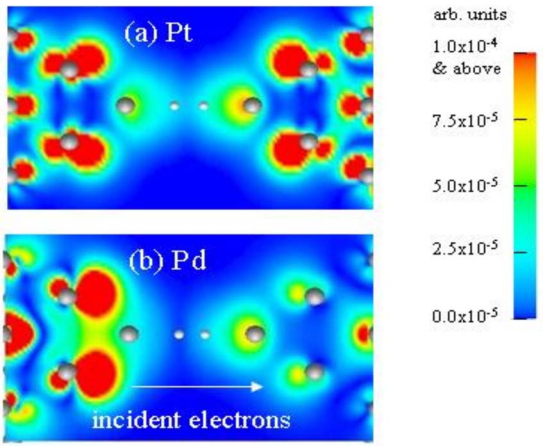

FIG. 3. (Color online) Color contour plot of square of conducting eigenchannel wave function with the highest eigenvalue at E_F in a plane containing the H_2 molecule for the (a) Pt-H_2 and (b) Pd-H_2 systems, overlaid on a ball-and-stick model of the atomic positions. Scattering states are incident from the left, and these results are obtained from Γ-point calculations.

In Fig. 4(a), we compare the PDOS of the transmitting eigenchannel wave function on the extended molecule with the PDOS in the bulk lead of the Pt-H_2 system. To better understand the features observed in the transmission and how they relate to the PDOS, we consider a simple one-dimensional tight-binding model of a symmetric single-channel junction, consisting of two semi-infinite leads coupled to a single impurity level, as a function of the lead-impurity coupling (details in the Appendix). For strong lead-impurity coupling, the impurity state broadens into a featureless resonance, except for van Hove singularities at energies close to the lead band edges. This results in a *plateau* of unit transmission and ballistic behavior over an energy range given by the lead bandwidth. We refer to this situation, where the PDOS is relatively featureless but the conductance is unity, as the bandlike regime. As the lead-impurity coupling is reduced, however, the PDOS and transmission spectrum due to the impurity resonance will take the form of a peak with a width proportional to the electronic coupling,

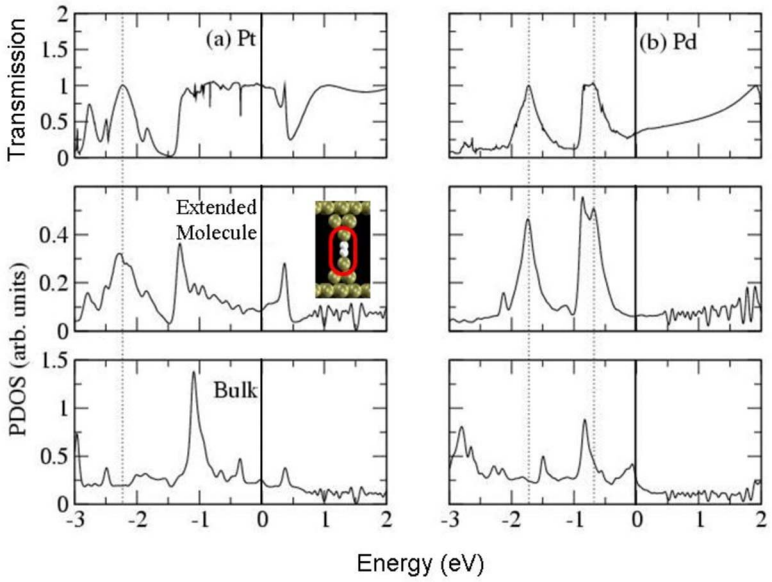

FIG. 4. (Color online) Transmission and conducting eigenchannel density of states obtained from a Γ-point calculation projected onto the extended molecule and deep inside the lead for (a) Pt-H_2 and (b) Pd-H_2 systems. Dotted lines centered on resonant-tunneling peaks serve as a guide to the eye and the Fermi level is at the zero of energy; the inset shows the region of projection for extended molecule PDOS.

and we refer to this case as the resonant-tunneling regime.

For the Pt-H_2 junction, there are peaks visible in the extended molecule PDOS in Fig. 4(a) at energies −2.3 and −1.3 eV (relative to the Fermi energy). The −2.3 eV peak directly corresponds to a feature in the transmission, and it is absent in the bulk-lead PDOS, indicating that it is derived from resonant states localized in the junction region. The −1.3 eV PDOS also has a corresponding feature in the transmission spectrum, but this feature is directly adjacent to and blends into the broad, bandlike plateau transmission feature that extends from −1.1 eV to energies above the range of our transmission spectrum. The onset of the broad transmission plateau at −1.1 eV is correlated with the peaked feature in the bulk PDOS at ∼−1.1 eV, which is associated with a band-edge van Hove singularity. For energies above this band edge, the coupling of the Pt 6*s* states to the extended molecule is strong enough to give rise to a plateau in transmission. The Pd-H_2 junction transmission, in contrast, exhibits just two dominant peaks, at −1.7 and −0.7 eV, which are well aligned with corresponding peaks in the extended molecule PDOS, indicative of off-resonance tunneling behavior.

Our analysis above suggests a large difference in coupling strength between the Pt-H_2 and Pd-H_2 junctions. To quantitatively investigate this issue, we calculate the hopping parameter γ_i, defined as $\langle i|H|\varphi\rangle$, where H is the Hamiltonian, $|i\rangle$ are basis orbitals on pyramid base atoms adjacent to the extended molecule, and $|\varphi\rangle$ is the eigenstate of the extended molecule dominating conduction close to the Fermi level. For Pt-H_2 junctions, we obtain $\gamma_s=1.05$ eV, $\gamma_{p_z}=1.21$ eV, and $\gamma_{d_z^2}=0.59$ eV, and for Pd-H_2, junctions $\gamma_s=0.39$ eV, $\gamma_{p_z}=0.72$ eV, and $\gamma_{d_z^2}=0.48$ eV. The hopping parameters in the Pt-H_2 system are larger than those in the Pd-H_2 system for states around E_F, as expected. The reason for a greater coupling for Pt is that in the extended molecule eigenstate $|\varphi\rangle$, the Pt tip atoms have more *s*-orbital weight close to E_F, whereas the Pd tip atoms possess more d_z^2-orbital character, which is significantly shorter ranged. The *s*-like orbital on the tip atom results in more overlaps with the orbitals in the metallic contacts, leading to a larger hopping matrix element. The increased *s*-orbital character on the Pt tip atoms is consistent with the ground-state electronic configuration of isolated Pt atoms, which is d^9s^1, compared with that in Pd atoms given by d^{10}.

Finally, to illustrate the role of the tip atoms in determining the junction conductance, we repeat the transmission calculation for the Pd extended molecule connected *to Pt leads*; the results appear in Fig. 5.

Notice that after this replacement, the conductance drops considerably and the transmission spectrum resembles that of the Pd system, with localized resonances appearing near E_F. Similarly, for the case of the Pt extended molecule with Pd leads, we observe a transmission plateau near E_F, similar to the Pt system [Fig. 5(b)]. This clearly demonstrates that the transmission is dominated by the nature of the extended molecule in both systems.

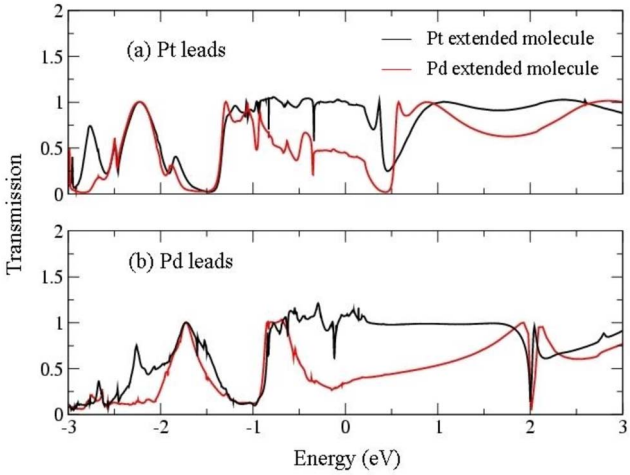

FIG. 5. (Color online) Transmission spectra obtained from Γ-point calculations for Pt extended molecule (black) and Pd extended molecule (red) across (a) Pt leads and (b) Pd leads.

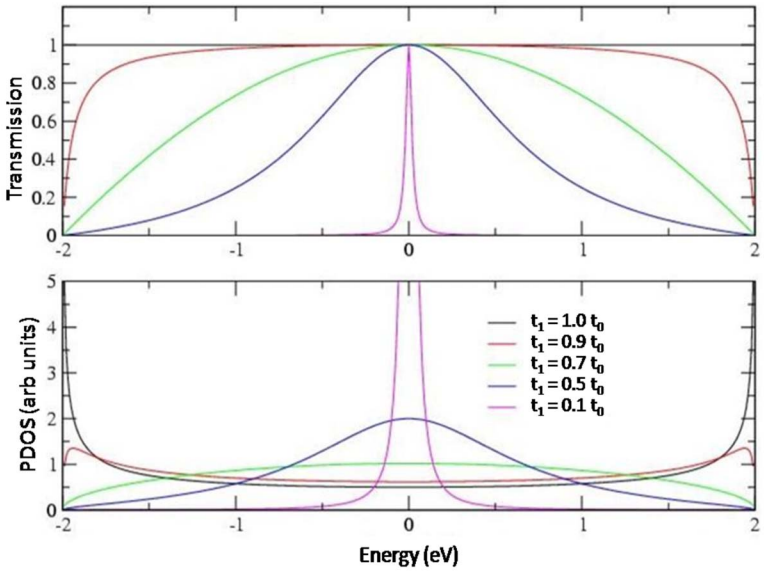

FIG. 6. (Color online) Transmission and impurity PDOS as a function of energy for a single state impurity tight-binding model with $t_0=1$ for a range of values of t_1.

V. CONCLUSION

To conclude, we have performed first-principles conductance calculations on junctions with H_2 placed between Pt and Pd pyramid tips connected to planar (111) leads and have obtained zero-bias conductance values in agreement with experiment.[27,28] This agreement suggests that correlation effects, which are believed to contribute to differences between calculated and measured conductances in many organic molecules, may play a less important role for H_2 junctions with Pt or Pd leads.[9–11] We also showed that there is a single-channel transmission over a wide energy range independent of the lead chemistry and demonstrated that the nature of transmission about E_F for Pt-H_2 and Pd-H_2 junctions is dominated by a four atom extended molecule, consisting of the H_2 molecule plus two adjacent metal tip atoms. The dramatic difference in zero-bias conductances is explained in terms of a difference in conduction mechanism, arising from stronger coupling between the contacts and the extended molecule in the Pt system relative to the Pd one, giving rise to zero-bias conductances in the ballistic and off-resonant-tunneling regimes for Pt-H_2 and Pd-H_2 junctions, respectively.

ACKNOWLEDGMENTS

We would like to thank Young-Woo Son for numerous valuable discussions. This work was supported by National Science Foundation Grant No. DMR04-39768 and DMR07-05941. Portions of this work were also performed at the Molecular Foundry, Lawrence Berkeley National Laboratory and were supported by the Office of Science, Office of Basic Energy Sciences of the U.S. Department of Energy under Contract No. DE-AC02-05CH11231. Computational resources have been provided by the National Energy Research Scientific Computing Center and the San Diego Supercomputing Center.

APPENDIX

Our tight-binding model consists of two semi-infinite one-dimensional leads coupled to a single impurity state. The lead atoms have a single orbital basis and a nearest-neighbor coupling strength of t_0, while the lead-impurity coupling is t_1. The Hamiltonian is given by

$$\mathrm{H} = \left(-t_0 \sum_{i=-\infty}^{-1} c_{i-1}^{+} c_i - t_0 \sum_{i=1}^{\infty} c_i^{+} c_{i+1} - t_1 (c_0^{+} c_{-1} + c_0^{+} c_1) \right) + \text{c.c.}$$

The following are expressions derived for the transmission $T(E)$ and projected density of states on the impurity $\rho_{impurity}(E)$ as a function of energy (Fig. 6).

$$T(E) = \frac{1 - \dfrac{E^2}{4t_0^2}}{1 + (\alpha^4 - 2\alpha^2)\dfrac{E^2}{4t_0^2}},$$

$$\rho_{impurity}(E) = \frac{1}{4\pi t_0} \frac{T(E)\alpha^2}{\sqrt{1 - \dfrac{E^2}{4t_0^2}}},$$

where $\alpha = t_0/t_1$.

[1] J. Reichert, R. Ochs, D. Beckmann, H. B. Weber, M. Mayor, and H. v. Lohneysen, Phys. Rev. Lett. **88**, 176804 (2002).
[2] M. Elbing, R. Ochs, M. Koentopp, M. Fischer, C. von Hanisch, F. Weigend, F. Evers, H. B. Weber, and M. Mayor, Proc. Natl. Acad. Sci. U.S.A. **102**, 8815 (2005).
[3] C. Untiedt, D. M. T. Dekker, D. Djukic, and J. M. van Ruitenbeek, Phys. Rev. B **69**, 081401(R) (2004).
[4] N. P. Guisinger, N. L. Yoder, and M. C. Hersam, Proc. Natl. Acad. Sci. U.S.A. **102**, 8838 (2005).
[5] B. Q. Xu and N. J. J. Tao, Science **301**, 1221 (2003).
[6] L. Venkataraman, J. E. Klare, C. Nuckolls, M. S. Hybertsen, and M. L. Steigerwald, Nature (London) **442**, 904 (2006).
[7] L. Venkataraman, J. E. Klare, I. W. Tam, C. Nuckolls, M. S. Hybertsen, and M. L. Steigerwald, Nano Lett. **6**, 458 (2006).
[8] S. Y. Jang, P. Reddy, A. Majumdar, and R. A. Segalman, Nano Lett. **6**, 2362 (2006).
[9] S. A. Getty, C. Engtrakul, L. Wang, R. Liu, S. H. Ke, H. U. Baranger, W. Yang, M. S. Fuhrer, and L. R. Sita, Phys. Rev. B **71**, 241401(R) (2005).
[10] K. Stokbro, J. Taylor, M. Brandbyge, J. L. Mozos, and P. Ordejon, Comput. Mater. Sci. **27**, 151 (2003).
[11] M. Di Ventra, S. T. Pantelides, and N. D. Lang, Phys. Rev. Lett. **84**, 979 (2000).
[12] S. Csonka, A. Halbritter, G. Mihaly, E. Jurdik, O. I. Shklyarevskii, S. Speller, and H. van Kempen, Phys. Rev. Lett. **90**, 116803 (2003).
[13] R. H. M. Smit, C. Untiedt, G. Rubio-Bollinger, R. C. Segers, and J. M. van Ruitenbeek, Phys. Rev. Lett. **91**, 076805 (2003).
[14] C. Untiedt, A. I. Yanson, R. Grande, G. Rubio-Bollinger, N. Agrait, S. Vieira, and J. M. van Ruitenbeek, Phys. Rev. B **66**, 085418 (2002).
[15] N. Agrait, A. L. Yeyati, and J. M. van Ruitenbeek, Phys. Rep. **377**, 81 (2003).
[16] A. I. Yanson, G. Rubio Bollinger, H. E. van den Brom, N. Agrait, and J. M. van Ruitenbeek, Nature (London) **395**, 783 (1998).
[17] C. Toher, A. Filippetti, S. Sanvito, and K. Burke, Phys. Rev. Lett. **95**, 146402 (2005).
[18] A. Ferretti, A. Calzolari, R. Di Felice, F. Manghi, M. J. Caldas, M. B. Nardelli, and E. Molinari, Phys. Rev. Lett. **94**, 116802 (2005).
[19] N. Sai, M. Zwolak, G. Vignale, and M. Di Ventra, Phys. Rev. Lett. **94**, 186810 (2005).
[20] J. B. Neaton, M. S. Hybertsen, and S. G. Louie, Phys. Rev. Lett. **97**, 216405 (2006).
[21] M. Koentopp, K. Burke, and F. Evers, Phys. Rev. B **73**, 121403(R) (2006).
[22] X. J. Wu, Q. X. Li, and J. L. Yang, Phys. Rev. B **72**, 115438 (2005).
[23] V. M. Garcia-Suarez, A. R. Rocha, S. W. Bailey, C. J. Lambert, S. Sanvito, and J. Ferrer, Phys. Rev. B **72**, 045437 (2005).
[24] K. S. Thygesen and K. W. Jacobsen, Phys. Rev. Lett. **94**, 036807 (2005).
[25] J. C. Cuevas, J. Heurich, F. Pauly, W. Wenzel, and G. Schon, Nanotechnology **14**, R29 (2003).
[26] Y. Garcia, J. J. Palacios, E. SanFabian, J. A. Verges, A. J. Perez-Jimenez, and E. Louis, Phys. Rev. B **69**, 041402(R) (2004).
[27] R. H. M. Smit, Y. Noat, C. Untiedt, N. D. Lang, M. C. van Hemert, and J. M. van Ruitenbeek, Nature (London) **419**, 906 (2002).
[28] S. Csonka, A. Halbritter, G. Mihaly, O. I. Shklyarevskii, S. Speller, and H. van Kempen, Phys. Rev. Lett. **93**, 016802 (2004).
[29] H. J. Choi, M. L. Cohen, and S. G. Louie, Phys. Rev. B **76**, 155420 (2007).
[30] W. Kohn and L. J. Sham, Phys. Rev. **140**, 1133 (1965).
[31] D. M. Ceperley and B. J. Alder, Phys. Rev. Lett. **45**, 566 (1980).
[32] E. Artacho, D. Sanchez-Portal, P. Ordejon, A. Garcia, and J. M. Soler, Phys. Status Solidi B **215**, 809 (1999).
[33] J. M. Soler, E. Artacho, J. D. Gale, A. Garcia, J. Junquera, P. Ordejon, and D. Sanchez-Portal, J. Phys.: Condens. Matter **14**, 2745 (2002).
[34] N. Troullier and J. L. Martins, Phys. Rev. B **43**, 1993 (1991).
[35] J. B. Neaton, K. H. Khoo, C. D. Spataru, and S. G. Louie, Comput. Phys. Commun. **169**, 1 (2005).
[36] J. K. Tomfohr and O. F. Sankey, Phys. Rev. B **65**, 245105 (2002).
[37] S. Datta, *Electronic Transport in Mesoscopic Systems* (Cambridge University Press, Cambridge, England, 1995).
[38] H. Ohnishi, Y. Kondo, and K. Takayanagi, Nature (London) **395**, 780 (1998).
[39] E. Z. da Silva, A. J. R. da Silva, and A. Fazzio, Phys. Rev. Lett. **87**, 256102 (2001).
[40] P. J. Feibelman, Phys. Rev. B **56**, 2175 (1997).
[41] M. Methfessel, D. Hennig, and M. Scheffler, Phys. Rev. B **46**, 4816 (1992).
[42] M. Brandbyge, M. R. Sorensen, and K. W. Jacobsen, Phys. Rev. B **56**, 14956 (1997).
[43] J. C. Cuevas, A. L. Yeyati, and A. Martin-Rodero, Phys. Rev. Lett. **80**, 1066 (1998).
[44] S. Datta and W. D. Tian, Phys. Rev. B **55**, R1914 (1997).
[45] The phase shift at any given energy is proportional to the difference between the energy integral of the even and odd projected densities of states. The transmission converges to the scattering-state formalism results if the projection space encompasses all regions relevant to electron scattering.